Biochemical Pharmacology 83 (2012) 893–902

Contents lists available at SciVerse ScienceDirect

Biochemical Pharmacology

journal homepage: www.elsevier.com/locate/biochempharm

Stereoisomers ginsenosides-20(S)-Rg_3 and -20(R)-Rg_3 differentially induce angiogenesis through peroxisome proliferator-activated receptor-gamma

Hoi-Hin Kwok [a], Guan-Lun Guo [b], Justin Kai-Chi Lau [b], Yuen-Kit Cheng [b], Jiang-Rong Wang [c], Zhi-Hong Jiang [c], Man-Hong Keung [a], Nai-Ki Mak [a], Patrick Ying-Kit Yue [a], Ricky Ngok-Shun Wong [a,*]

[a] Department of Biology, Faculty of Science, Hong Kong Baptist University, Hong Kong
[b] Department of Chemistry, Faculty of Science, Hong Kong Baptist University, Hong Kong
[c] Center for Cancer and Inflammation Research, School of Chinese Medicine, Hong Kong Baptist University, Hong Kong

ARTICLE INFO

Article history:
Received 10 November 2011
Accepted 27 December 2011
Available online 4 January 2012

Keywords:
Ginsenoside
Rg_3
Stereoisomer
Angiogenesis
PPARγ

ABSTRACT

Ginsenosides are considered the major constituents that are responsible for most of the pharmacological actions of ginseng. However, some ginsenosides exist as stereoisomeric pairs, detailed and molecular exposition based on the structural differences of ginsenoside stereoisomers has not been emphasized in most studies. Here we explore the functional differences of ginsenoside Rg_3 stereoisomers on angiogenesis. In this study, we demonstrated the distinctive differential angiogenic activities of 20(S)-Rg_3 and 20(R)-Rg_3 stereoisomers. 20(S)-Rg_3 at micromolar concentration promotes human endothelial cells proliferation, migration and tube formation *in vitro*, as well as *ex vivo* endothelial sprouting. The effects induced by 20(S)-Rg_3 are significantly more potent than 20(R)-Rg_3. These effects are partially mediated through the activation of AKT/ERK-eNOS signaling pathways. Moreover, knockdown of peroxisome proliferator-activated receptor-gamma (PPARγ) by specific small interference RNA abolished the 20(S)-Rg_3-induced angiogenesis, indicating that PPARγ is responsible for mediating the angiogenic activity of Rg_3. Using reporter gene assay, the PPARγ agonist activity of 20(S)-Rg_3 has been found 10-fold higher than that of 20(R)-Rg_3. Computer modeling also revealed the differential binding is due to the chiral center of 20(S)-Rg_3 can form a critical hydrogen bond with Tyr473 of PPARγ ligand binding domain. The present study elucidated the differential angiogenic effects of Rg_3 stereoisomers by acting as agonist of PPARγ. The results shed light on the structural difference between two ginsenoside stereoisomers that can lead to significant differential physiological outcomes which should be carefully considered in the future development of ginsenoside-based therapeutics.

1. Introduction

Panax ginseng C.A. Meyer is among the most popular herbal medicines widely used as general tonic to improve health and vitality. Ginsenosides are the pharmacological active phytochemicals of ginseng which belong to a family of triterpenoid saponins. Three types of ginsenosides have been classified, they are protopanaxadiols (e.g., Rb_1, Rb_2, and Rh_2), protopanaxatriols (e.g., Re, Rg_1 and Rg_2), and oleanolic acid derivatives [1]. Depending on the processing methods, composition of ginsenosides in ginseng may be altered; steaming of fresh ginseng for 2–3 h produces red ginseng with enrichment of several ginsenoside species such as Rg_3 which may increase from 0.37% to 1.32% (w/w) [2]. Structurally, ginsenosides contain a hydrophobic triterpenoid skeleton attached with hydrophilic sugar moieties or hydroxyl groups at carbon-3, -6 and -20. Protopanaxadiol-type ginsenosides 20(S)-Rg_3 and 20(R)-Rg_3 are enantiomeric pair that differ in the spatial orientation of hydroxyl group on the chiral center at carbon-20 (C20) (Fig. 1A and B). The major ginsenosides, such as Rb_1, Rb_2, and Rd can be readily converted into mixture of 20(S)-Rg_3 and 20(R)-Rg_3 stereoisomers by either acid treatment or heating, but the isolation of each isomer from the mixture is rather difficult [3]. Indeed, ginsenosides Rg_2, Rg_3, Rh_1, Rh_2, and Rs_3 all exist as stereoisomer pairs. Although stereoselectivity of ginsenosides on ion channel [4], effects on coronary artery contractions [5], anti-tumor effects [6], osteoclastgenesis inhibition [7], and endothelial cell apoptosis [8], have been described previously; detailed and molecular exposition based on the structural difference of ginsenoside stereoisomers have not been emphasized.

The mechanistic action of ginsenoside has been firstly suggested that Rg_1 can interact with glucocorticoid receptor [9]. After that, other ginsenosides such as Rb_1 and Rg_3 were demonstrated to activate estrogen receptor [10], and peroxisome proliferator-activated receptor (PPAR) [11]. Nuclear receptors

* Corresponding author. Tel.: +852 3411 7057; fax: +852 3411 5995.
E-mail address: rnswong@hkbu.edu.hk (R.-S. Wong).

0006-2952/$ – see front matter © 2012 Elsevier Inc. All rights reserved.
doi:10.1016/j.bcp.2011.12.039

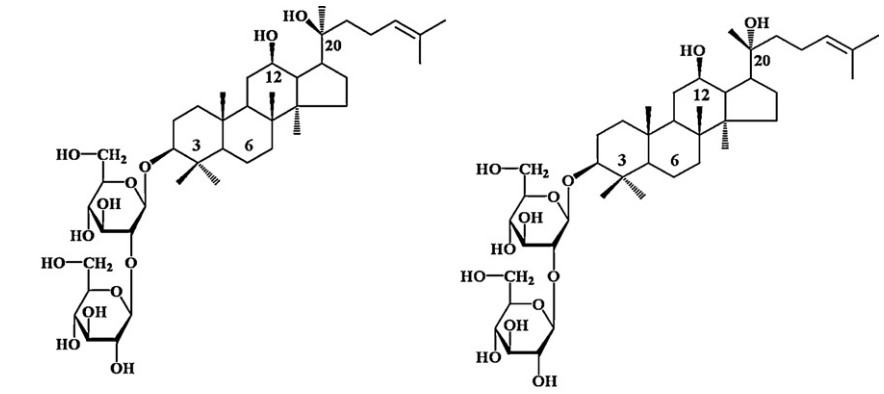

Fig. 1. Chemical structures of ginsenoside (A) 20(S)-Rg_3 and (B) 20(R)-Rg_3.

belong to a class of ligand dependent transcriptional factors which regulate diverse physiological functions. The endogenous ligands of PPARγ are polyunsaturated fatty acids. PPARs control many important metabolic functions, and PPARγ is the best-studied member of the family. PPARγ is predominantly expressed in adipocytes and some other metabolically active tissues. It is also initially found to be critical in lipid homeostasis and adipocyte differentiation [12]. Recent studies have implied the role of PPARγ in regulating angiogenesis. The commercially available anti-diabetic drug rosiglitazone, which is a PPARγ agonist, can increase endothelial progenitor cells functions by upregulating the AKT-eNOS signaling pathway [13]. Rosiglitazone also promotes angiogenesis and increases eNOS expression in endothelial cell after focal cerebral ischemia [14]. Similarly, prolonged treatment with troglitazone, another PPARγ agonist, increases endothelial nitric oxide (eNOS) production through PPARγ-dependent signaling pathway [15]. These studies highlighted the possible role of PPARγ on angiogenesis.

Angiogenesis is defined as the formation of new blood capillaries from pre-existing vascular networks [16]. It is an essential physiological process during embryogenesis, pregnancy and wound healing. Besides, angiogenesis is also contributed to the pathogenesis of diabetic retinopathy, rheumatoid arthritis and tumor development [17]. Distinct but tightly regulated events are involved during angiogenesis, including degradation of extracellular matrix, proliferation, migration of endothelial cells, and formation of capillary lumen. In the present study, we presented evidences to support the differential angiogenic properties of Rg_3 stereoisomers at micromolar level on human endothelial cells. In addition, we identified PPARγ as the molecular target which mediated the differential actions of Rg_3 stereoisomers.

2. Materials and methods

2.1. Materials

Ginsenosides 20(S)-Rg_3 and 20(R)-Rg_3 with purity about 98% were obtained from Fleton (Chengdu, China). Anti-phospho eNOS (S1177), anti-phospho AKT (S473), anti-AKT, anti-phospho ERK (T202/Y204) and anti-ERK antibodies were obtained from Cell Signaling Technology (Beverly, MA, USA). Anti-actin antibody was purchased from Sigma–Aldrich (St. Louis, MO, USA). Anti-eNOS antibody was obtained from Upstate (Waltham, MA, USA). Horseradish peroxidase-conjugated (HRP)-conjugated secondary antibodies were purchased from Zymed (South San Francisco, CA, USA). PPARs lignads were purchased from Tocris Biosciences (Ellisville, MO, USA).

2.2. Analyses of ginsenosides by UPLC-MS

Analyses of ginsenoside Rg_3 stereoisomers were carried out on a Waters ACQUITY UPLC™ system (Waters Corp., MA, USA) which was equipped with a binary solvent delivery system and a sample manager coupled to Bruker MicroTOF mass spectrometer with an ESI source. The chromatography was performed on an Acquity BEH C_{18} column (2.1 mm × 100 mm, 1.7 μm). The mobile phase is consisted of water containing 0.1% formic acid (A) and acetonitrile containing 0.1% formic acid (B). Optimized UPLC elution condition as following was employed: linear gradient from 28% to 55% B at 0–15 min, then increase to 70% B at 15–19 min, and finally from 70 to 100% B at 19–19.5 min. The ESI-MS data were acquired in negative mode and conditions for MS analysis were as follows: end plate offset, −500 V; capillary voltage, 4500 V; nebulizing gas (N_2) pressure, 1.5 bar; drying gas (N_2) flow rate, 8.0 l/min; drying gas temperature, 200 °C; mass range, m/z 300–1500.

2.3. Cell culture and treatment

Human umbilical vein endothelial cells (HUVECs) and human neonatal dermal fibroblasts (HDFs) were obtained from Lonza (Walkersville, MD, USA) and were maintained in passages 2–8 to ensure genetic stability. HUVECs were cultured in M199 medium supplemented with heparin (90 mg/l), heat-inactivated FBS (20%, v/v), ECGS (20 μg/ml), and PS (1%, v/v), HDFs were cultured in DMEM supplemented with FBS (10%, v/v) and penicillin/steptomycin (1%, v/v) and kept at 37 °C in a humidified 5% CO_2 incubator. HUVECs were seeded and treated with ginsenoside Rg_3 in M199 containing 1% FBS. Ginsenosides were obtained from Fleton (Chengdu, China) with purity over 98%.

2.4. Cell proliferation assay

HUVECs (1×10^4 cells/well) were seeded onto 96-well plates overnight. After drug treatment for the indicated time, cell proliferation was determined by the (3-(4,5-dimethylthiazol-2-yl)-2,5-diphenyltetrazolium bromide (MTT) assay and bromodeoxyuridine (BrdU) incorporation ELISA. The MTT assay was based on the cleavage of the yellow tetrazolium salt to purple formazan crystal by living cells. Briefly, cells were incubated with MTT solution (0.5 mg/ml) in assay medium for 4 h. The formazan product was solubilized by DMSO after complete removal of medium; absorbance at wavelength 540 nm and 690 nm (reference) was measured by the microplate reader (Infinite F200, Tecan, Männedorf, Switzerland). Cell proliferation was also determined using BrdU incorporation kit (Roche Biochemicals, Milan, Italy).

The cells were labeled with BrdU (10 μM) for 2 h according to the manufacturer's protocol. Absorbance at 450 nm was measured by microplate reader.

2.5. Cell migration assay

HUVECs (3×10^4 cells/well) were seeded onto 96-well plates overnight. An artificial wound was created by mechanical scratching of the cell monolayer using home-made mechanical wounder [18]. The sharp wound image in each well was captured. Culture medium was replaced with fresh medium containing ginsenoside Rg_3 (0.01–30 μM), cells were then incubated for further 24 h and the wounded area of each well was captured again. Images at 0 and 24 h were analyzed using ImageJ software (http://rsb.onfo.nih.gov). The migration of cells towards the denuded area was expressed as percentage of recovery. Percentage of recovery = $A_{t0} - A_{t24}/A_{t0} \times 100\%$ where A_{t0} is the wounded area measured immediately after scratching, A_{t24} is the wounded area measured 24 h after wounding.

2.6. Capillary-like tube formation assay

The 96-well plate precoated with growth factor reduced-Matrigel (BD Bioscience, San Jose, CA, USA) was allowed to solidify at 37 °C for 1 h. HUVECs were then plated in the presence or absence of ginsenoside in 1% FBS supplemented medium. Images of each well were captured after 24 h. The angiogenic activities were determined by counting the branch points of formed tubes in each well.

2.7. Aortic ring sprouting assay

The rat aortic rings were prepared and treated as described previously [19]. Briefly, aortic fragments were first isolated from rat, and were sandwiched between two layers of growth factor reduced Matrigel™ matrix in 96-well plate. The cultures were incubated in 200 μl endothelial growth medium containing ECGS (200 mg/ml) or Rg_3 stereoisomers. Culture medium was refreshed on day 4 and the microvascular outgrowths were determined according to their morphology. Images were captured using stereomicroscope (Olympus SZX16) attached with a digital camera (Olympus DP71) (Olymus America Inc).

2.8. Western blot analysis

Treated or untreated cells were washed with ice-cold PBS twice, and were lysed by ice-cold cell lysis buffer (Novagen, USA) supplemented with protease inhibitor cocktail (1%, v/v) and phosphatase inhibitor cocktail (0.5%, v/v) (Calbiochem, San Diego, CA, USA). The cells were scraped off by rubber policeman, and the protein in the supernatant was collected after centrifugation. The concentration of protein was determined by Dc protein assay (Bio-Rad, Hercules, CA, USA). Equal amount of protein was separated by 10% SDS-PAGE followed by electroblotting onto nitrocellulose transfer membrane. The membrane blocked with blocking buffer was then incubated with primary antibodies. The washed membrane was then further incubated with horseradish peroxidase-conjugated goat-anti-rabbit IgG or horseradish peroxidase-conjugated goat-anti-mouse IgG (Invitrogen). The protein band was visualized by Chemiluminescent Western Detection Kit (Bio-Rad). Band intensities from triplicate were quantitatively analyzed by ImageJ software.

2.9. PPARγ time-resolved fluorescence resonance energy transfer (TR-FRET) competitive binding assay

PPARγ LanthaScreen™ TR-FRET competitive binding assay (Invitrogen) was used to study the binding between ginsenosides Rg_3 and PPARγ. This assay allowed screening of ligands for PPARγ. The method is based on the principle that when two suitable fluorophores are brought together in close proximity, excitation of the fluorophore can result in energy transfer to the acceptor fluorophore which can be monitored readily. In this assay, the GST-tagged PPARγ-ligand binding domain (LBD) was combined with terbium-labeled anti-GST antibody. When a green fluorescent pan-PPAR ligand (tracer) is bound to the receptor, energy transfer from the antibody to the tracer occurs, and a high TR-FRET ratio is observed. The ability of GW1929 (1 pM–100 μM), a PPARγ specific agonist, and ginsenoside Rg_3 (10 nM–100 μM) to displace the tracer from LBD was tested, which resulted in a loss of FRET ratio.

2.10. PPARγ reporter gene assay

PPARγ reporter gene assay was performed in human dermal fibroblast (HDFs). Cells were seeded in 24-well plate overnight, then cells were starved in serum-free Opti-MEM for another 24 h and transiently transfected with reporter plasmid peroxisome proliferator-activated receptor response element (PPRE)X3-TK-luc (contains three copies of DR-1 response elements upstream of a luciferase reporter) (250 ng/well) (Addgene plasmid 1015), expression plasmids pSG5-PPARγ (125 ng/well) and pSG5-RXRα (125 ng/well) using Lipofectamine LTX transfection reagent (1.5 μl/well) (Invitrogen). After 6 h of transfection, cells were washed once with Opti-MEM and further incubated with troglitazone (PPARγ agonist) or ginsenosides for 24 h. Cells were lysed by passive reporter lysis buffer; luciferase activity was measured using Luciferase Assay System (Promega, Madison, WI, USA) with microplate luminometer (Tecan). Luciferase activity was normalized by the amount of protein in the cell lysate.

2.11. Small interference RNA transfection

Cells were transiently transfected with PPARγ-siRNA (50 nM) complexed with RNAiMAX transfection reagent (1.5 μl/well) (Invitrogen) in Opti-MEM for 24 h. Cells were rinsed with Opti-MEM followed by drug treatment. Non-sequence-specific negative control siRNA (Dharmacon, Lafayette, CO, USA) was used in parallel with PPARγ-siRNA.

2.12. Statistical analysis

All results were expressed as mean ± standard derivation (S.D.) of at least 3 independent experiments. Statistical differences between two groups were analyzed by unpaired Student's *t*-test.

3. Results

3.1. Characterization of Rg_3 stereoisomers by UPLC-MS

To demonstrate the purity of each ginsenoside Rg_3 stereoisomers, UPLC-MS was used. Under the optimized conditions mentioned in materials and methods, 20(S)-Rg_3 and 20(R)-Rg_3 can be separated with good resolution (Fig. 2B and C). 20(S)-Rg_3 and 20(R)-Rg_3 were characterized by comparing the values of UPLC retention time and MS spectra with those of the authentic standards.

3.2. Differential angiogenic effects of Rg_3 stereoisomers

Differential HUVECs proliferation was observed after treatment with ginsenosides-Rg_3 stereoisomers for 24 h. 20(S)-Rg_3 (15 μM) increased 50% of cell proliferation, while only 10% of cell proliferation was stimulated by the same concentration of 20(R)-Rg_3 (Fig. 3A). Furthermore, by using the BrdU incorporation

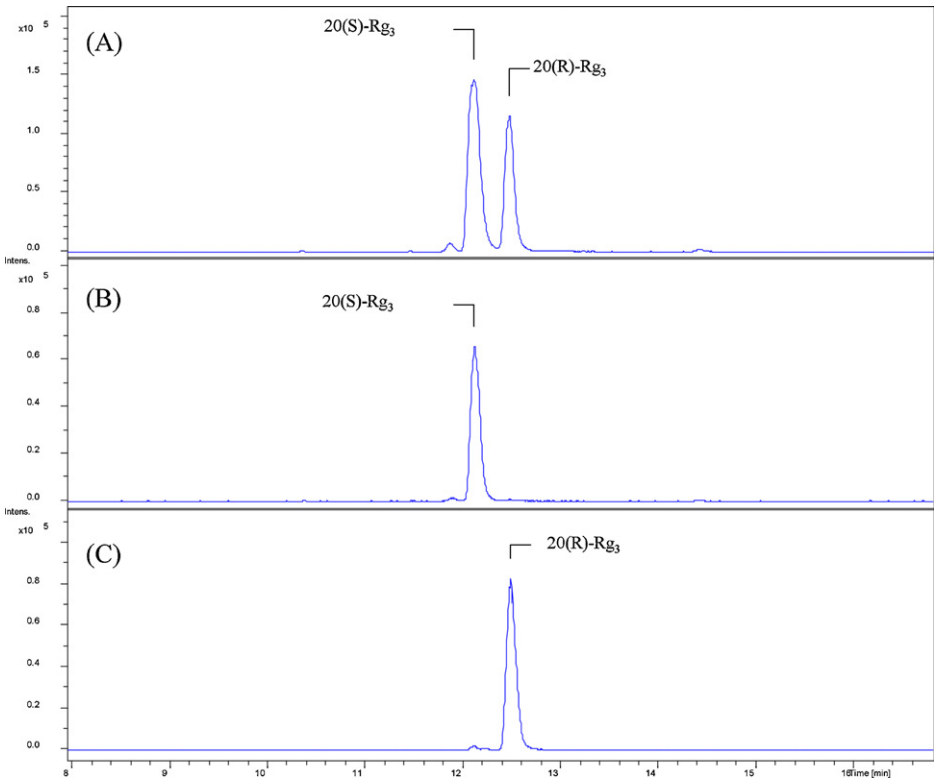

Fig. 2. UPLC-TOF-MS chromatograms of (A) stereoisomeric Rg_3, (B) 20(S)-Rg_3, and (C) 20(R)-Rg_3.

assay, which is a direct indicator for DNA synthesis during cell proliferation, 20(S)-Rg_3 (15 μM) stimulated HUVECs' DNA synthesis by 20%; while 20(R)-Rg_3 did not showed any inducing effect on HUVECs' DNA synthesis (Fig. 3B). Then the effect of Rg_3 stereoisomers on cell motility was further examined. As shown in Fig. 3C, only 20(S)-Rg_3 (15–30 μM) can increase endothelial cells migration, while 20(R)-Rg_3 exerted no significant effect on cell migration. In the tube formation assay, result showed that micromolar level of 20(R)-Rg_3 could also induce tubular network formation. However, the extent of tube formation was not as much as in the case of 20(S)-Rg_3, in which the average number of tube induced by 20(S)-Rg_3 was about 90, while in the case of 20(R)-Rg_3, it could only induce 60 tubes in each well (Fig. 3D). Furthermore, the differential angiogenic properties between 20(S)-Rg_3 and 20(R)-Rg_3 were further evaluated by *ex vivo* culturing of rat aortic rings; the endothelial cell sprouting. ECGS, as a positive control, induced microvascular sprouting when compared with untreated control; while 20(S)-Rg_3 (10 μM) can also increase microvascular sprouting but not for 20(R)-Rg_3 (Supplementary Fig. 1C). These findings demonstrated that 20(S)-Rg_3 at micromolar level is a lot more potent than 20(R)-Rg_3 in promoting angiogenesis.

3.3. 20(S)-Rg_3 activates AKT, ERK and eNOS to induce HUVECs proliferation

The signaling pathways activated by Rg_3 to induce angiogenesis were then studied. Rapid and sustained phosphorylation of ERK in HUVECs were found after 20(S)-Rg_3 (15 μM) treatment; whereas no effect was observed in 20(R)-Rg_3 treated cells (Fig. 4A). In addition, sequential increase of phosphorylation of AKT at Ser473 and eNOS at Ser1177 was found after 60 min of 20(S)-Rg_3 treatment. Again, 20(R)-Rg_3 did not show similar effect. Moreover, pretreatment with L-NAME, PD98059 and LY294002, which are the inhibitors of eNOS, ERK and PI3K, respectively, could partially but significantly abolish 20(S)-Rg_3-induced HUVECs proliferation (Fig. 4B), indicating that activation of eNOS, AKT and ERK were involved in 20(S)-Rg_3-induced HUVECs proliferation.

3.4. Rg_3 stereosiomers differentially activate PPARγ

To demonstrate that 20(S)-Rg_3 is a functional ligand of PPARγ, PPARγ luciferase reporter gene assay was performed. After treating HDFs with Rg_3 which have been transiently transfected with reporter plasmid containing PPRE, 20(S)-Rg_3 significantly increased luciferase activity in a dose-dependent manner (0.1–10 μM) which was comparable with troglitazone (5 μM). 20(R)-Rg_3 only induced 1.5-fold luciferase activity at 10 μM (Fig. 5). Therefore, the PPARγ transcriptional activity as activated by 20(S)-Rg_3 is about 10-times more potent than 20(R)-Rg_3. This suggested that the structural difference between 20(S)-Rg_3 and 20(R)-Rg_3 is critical for effective activation of PPARγ. To further examine the direct interaction of Rg_3 stereoisomers on PPARγ, time-resolved fluorescence resonance energy transfer (TR-FRET) screening assay was performed (Supplementary Fig. 2). However, due to the limited solubility of 20(R)-Rg_3 when concentration is higher than 100 μM, complete displacement of tracer from PPARγ-LBD was not observed in high 20(R)-Rg_3 concentration. In spite of the concentration limitation, 20(S)-Rg_3 can reduce the FRET ratio at lower concentration when compared with 20(R)-Rg_3. Moreover, computational modeling was used to delineate the binding mode of Rg_3 stereoisomers; the docking results suggest that both 20(R)-Rg_3 and 20(S)-Rg_3 occupy similar spatial position as that of rosiglitazone in the LBD of PPAR γ, at the C20 chiral center close to the helix-12, and their disaccharide groups are proximal to the β-sheet of the protein (Fig. 6). Furthermore, it can be seen that the hydroxyl group at the C20 chiral center of 20(S)-Rg_3 interacts with Tyr473 through hydrogen bond. Similar interaction is also observed in the crystal structure of PPARγ in complex with rosiglitazone in which the thiazole group form stable hydrogen bond to the side chain of Tyr473 (gray superposition) [20–22]. In

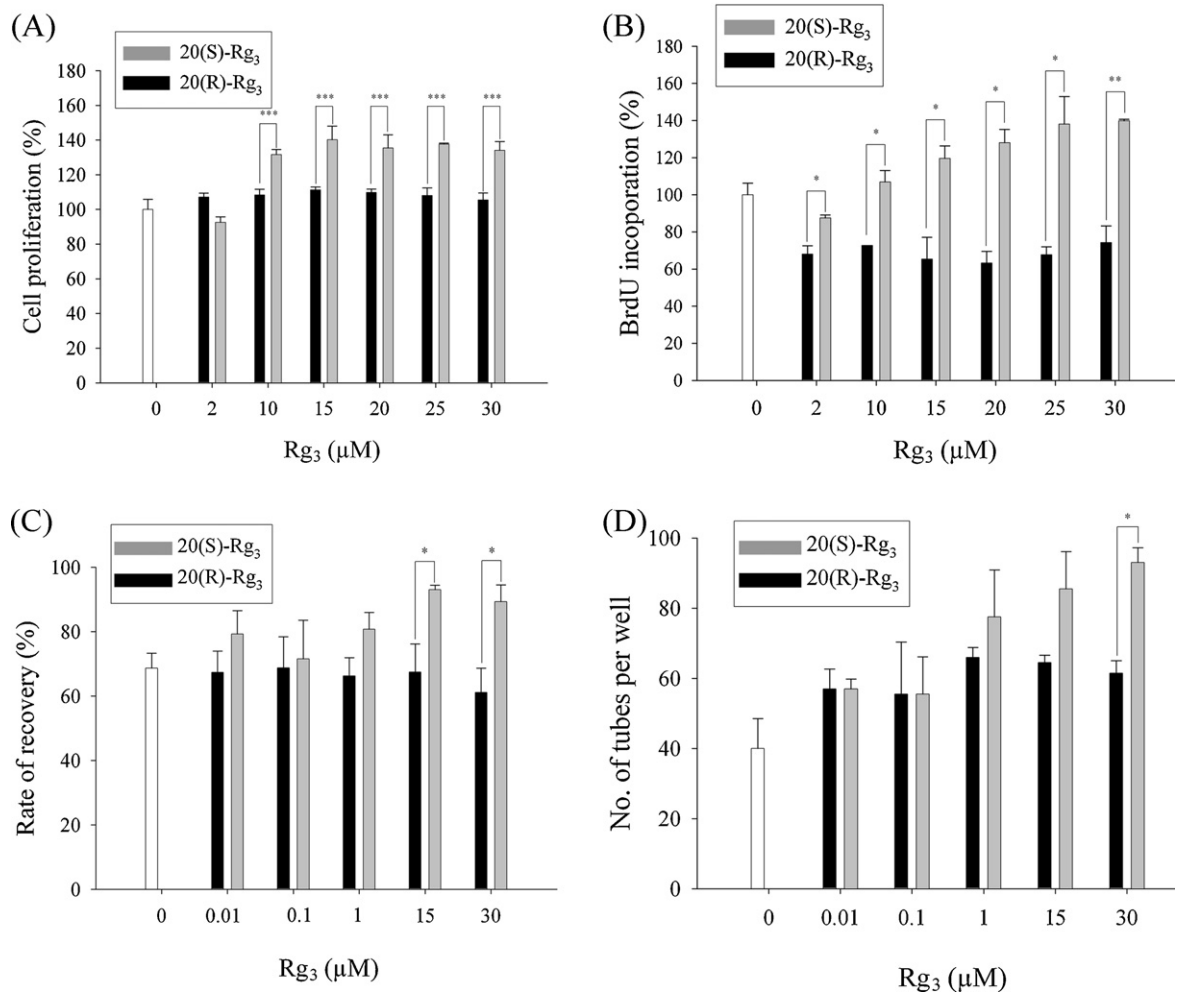

Fig. 3. Differential effects of Rg_3 stereoisomers on angiogenesis. HUVECs were treated with either form of Rg_3 stereoisomers for 24 h. Cell proliferation was determined by (A) MTT proliferation assay and (B) BrdU incorporation assay, values are expressed as the percentage of cell proliferation relative to the solvent control. (C) Rate of cell migration was determined as described in materials and methods. (D) Effect of tube formation after Rg_3 treatment, average number of tubes formed in each well. Values are presented as mean ± SD of three independent experiments. $^{*}p < 0.05$, $^{**}p < 0.01$, $^{***}p < 0.001$ vs DMSO control.

contrast, the sterically strained binding pocket does not allow the 20(R)-Rg_3 to interact optimally with Tyr473. Interaction with Tyr473 in helix-12 of PPARγ is required for the functional activity of full agonists. Mutation of Tyr473 to alanine abolishing the full agonistic activity of PPARγ [23]. The distinctive ligand-binding modes may contribute to the different binding affinity and the observed biological activity of the stereoisomers.

3.5. Angiogenic effects of Rg_3 is abolished by PPARγ-siRNA

To verify the role of PPARγ in Rg_3-induced angiogenesis, PPARγ-siRNA was used to deplete PPARγ expression (Fig. 7A). PPARγ-specific siRNA can significantly suppress 20(S)-Rg_3-induced HUVECs proliferation (Fig. 7B), migration (Fig. 7C) and tube formation (Fig. 7D). Activation of ERK/AKT/eNOS signaling pathway by 20(S)-Rg_3 was also largely reduced (Fig. 7E). In fact, only partial effect was found in 20(R)-Rg_3-treated cells. These results clearly demonstrated that PPARγ is essential for 20(S)-Rg_3-induced angiogenesis. In addition, the 20(S)-Rg_3-induced HUVECs proliferation, migration and eNOS, ERK, and AKT phosphorylation can also be inhibited by pretreatment with PPARγ-specific antagonist, GW9662 (Supplementary Fig. 3). Furthermore, pretreatment with PPARα or PPARβ/δ specific antagonists, GW6471 and GSK0660 (Supplementary Fig. 4A and B) exerted no inhibitory effect on Rg_3-induced HUVECs proliferation, which further confirmed that the specific role of PPARγ in Rg_3-induced angiogenesis.

4. Discussion

Ginsenosides account for most of the pharmacological effects of ginseng. Ginsenoside such as Rg_3 and Rh_2 have been suggested to possess anti-tumor and angiomodulatory activity [26,27]. The anti-inflammatory effects of Rh_1 [28], and neuroprotective effects of Rg_2 were also reported [29]. However, these ginsenosides can exist as stereoisomers. The importance of drug stereoselectivity is gaining greater attention in recent years [30], but little is known about the pharmacology of ginsenoside stereoisomers. Previous studies did not or rarely report the stereospecificity of the ginsenosides. The disregard of stereochemistry of ginsenosides may lead to disparate results *in vitro* when compared with *in vivo* assessments of potency [31–33]. It is because though the enantiomers of a ginsenoside possess the same functional group at C20, but the difference in three-dimensional structure may affect the binding affinity to the receptor binding site. It has been shown that 20(S)-Rh_2, the immediate metabolite of 20(S)-Rg_3, exhibits greater cellular uptake than 20(R)-Rh_2 properly due to greater affinity with stereospecific interaction with the ABC transporter [34]. In the present study, we have identified PPARγ as the molecular target which mediates the angiogenic effects of

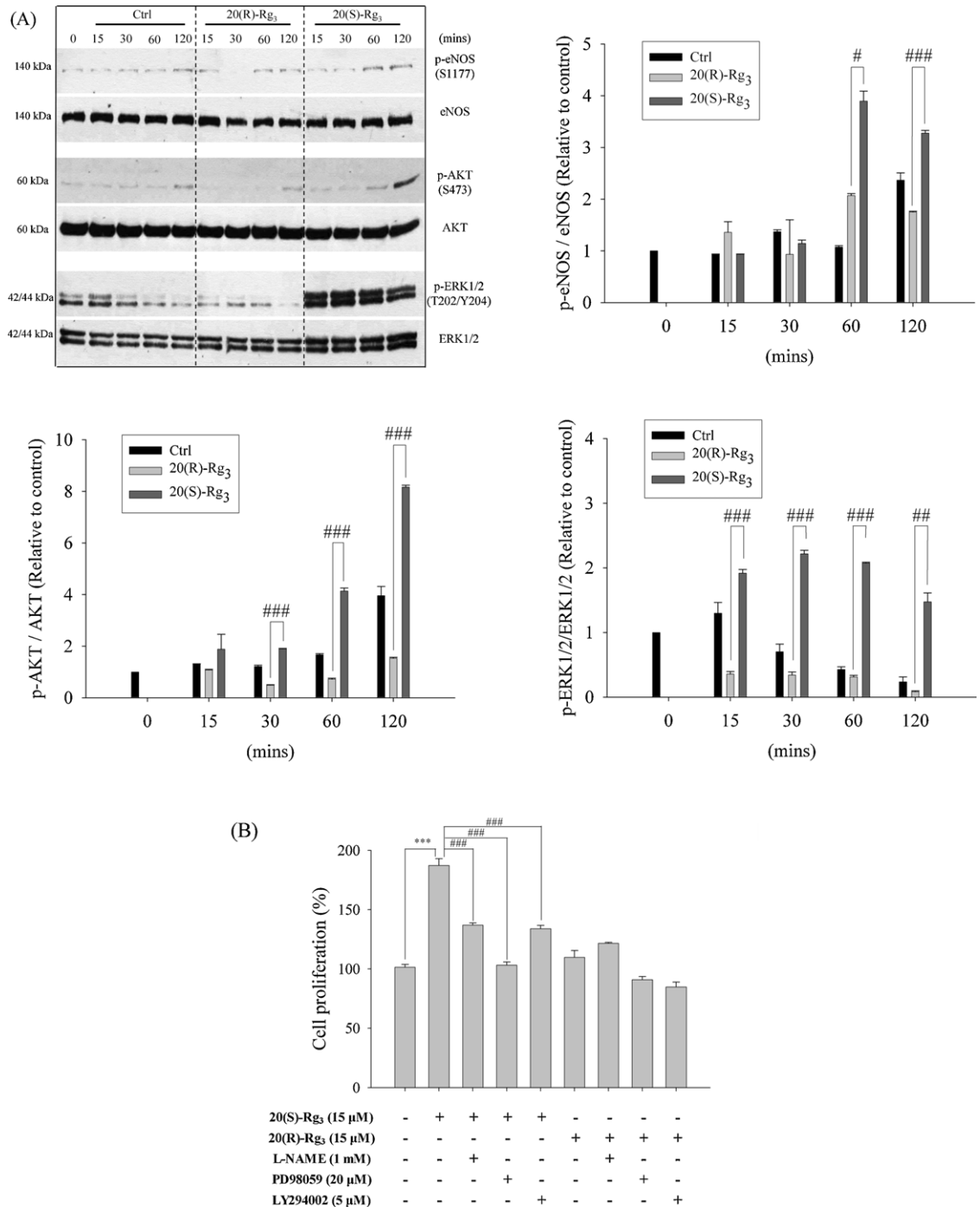

Fig. 4. Rg_3-induced proliferation of HUVECs is dependent on eNOS, AKT, and ERK1/2 activation. (A) Differential phosphorylation of eNOS, AKT, ERK. HUVECs were treated with either form of Rg_3 stereoisomers for the indicated time. Phosphorylated and total forms of eNOS, AKT and ERK were detected by Western blot analysis. Signal intensities were determined by quantitative densitometry and expressed as fold change of p-eNOS, p-AKT and p-ERK1/2 normalized to corresponding total form before compare with control. (B) Effects of various inhibitors on the proliferation of HUVECs. HUVECs were pretreated with indicated concentration of L-NAME (eNOS inhibitor), LY294002 (PI3K inhibitor), or PD98059 (ERK inhibitor) for 1 h, then co-incubated with either form of Rg_3 stereoisomers for another 24 h. Cell proliferation was determined by MTT proliferation assay. Values are presented as mean ± SD of three independent experiments. $^{***}p < 0.001$ vs DMSO control. $^{\#}p < 0.05$, $^{\#\#}p < 0.01$, $^{\#\#\#}p < 0.001$ vs 20(S)-Rg_3 treatment alone.

ginsenoside Rg_3 stereoisomers. PPAR ligands display a high degree of stereoselectivity [35]. In this report, we have also modeled that Tyr473 seems to be critical in distinguishing the differential pharmacological activity of the Rg_3 C20-enantiomers which corroborates with a recent novel polarization anisotropy study complemented with total internal reflection fluorescence microscopy technique [36]. This report clearly differentiated that only 20(S)-Rg3 but not 20(R)-Rg3 showed specific binding to PPARγ; although 20(S)-Rg3 showed only half of the binding affinity when compared with GW9662. On the other hand, from the results of reporter gene assay, both Rg_3 stereoisomers activate PPARγ transcription. However, 20(S)-Rg_3 is 10-fold more potent than 20(R)-Rg_3. This strongly implies that the C20 of Rg_3 is important for the binding of Rg_3 to PPARγ, in order to elicit downstream activities.

PPARγ has diverse roles relating to the regulation of glucose and lipid metabolism, inflammation, and immune responses. Ligands of PPARγ were reported to have both angiogenic and

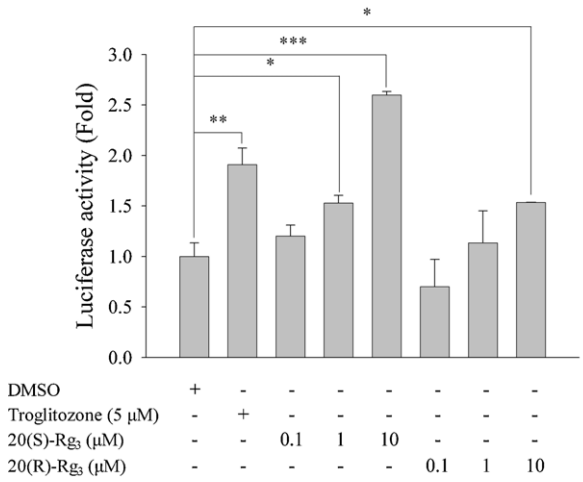

Fig. 5. Differential activation of PPARγ by stereoisomers of Rg_3. HDFs were transiently transfected with luciferase reporter plasmid containing three copies of PPRE together with PPARγ and RXRα expression plasmids. Luciferase reporter activity was measured 24 h after incubation of transfected cells with troglitazone and different concentrations of 20(S)-Rg_3 and 20(R)-Rg_3. Troglitazone was used as positive controls. Values are presented as mean ± SD of three independent experiments. $^{*}p < 0.05$, $^{**}p < 0.01$, $^{***}p < 0.001$ vs DMSO control.

anti-angiogenic effects depends on their interactions with co-activator and co-repressor [37]. Ginseng extract and ginsenosides are suggested to interact with PPARs in recent years. Among the thirty chemical variant of ginsenosides, Rf is the first being described to regulate lipoprotein metabolism through PPARα [38], several ginsenosides including Rg_3, Rh_2 and PPT are demonstrated to regulate adipogenesis by activating PPARγ and related signaling subsequently [11,39,40]. In fact, from the result of PPARγ reporter gene assay, 20(S)-Rg_3 can activate PPARγ at micromolar level. Although the binding affinity of 20(S)-Rg_3 is much lower than those of the synthetic agonists such as rosiglitazone (EC_{50} = 0.043 μM) and troglitazone (EC_{50} = 0.55 μM), 20(S)-Rg_3 may act as an herbal-base alternative of PPARγ agonist. As several reports have shown that rosiglitazone, which previously used for treating type II diabetes, may increase the risk of myocardial infraction and death from cardiovascular diseases [41]. So, a dietary supplement containing 20(S)-Rg_3 may act as an alternative or compensation of PPARγ agonist, which on one hand acts as PPARγ agonist, on the other hand, avoiding the adverse effects induced by those full agonists.

Rg_3 has been suggested to increase eNOS phosphorylation via estrogen receptor-dependent PI3K signaling [42]. In this report, we showed that ginsenoside Rg_3 differentially induces ERK/AKT-eNOS signaling pathways via activation of PPARγ, and induces HUVECs proliferation, migration, and tube formation. The ERK and AKT are upstream kinases which can phosphorylate eNOS at Ser1177 [43], the activation of ERK/AKT and eNOS by 20(S)-Rg_3 may enhance NO production and contribute to the rapid vasodilating effects of *P. ginseng* [44]. The phosphorylation of ERK/AKT-eNOS by Rg_3 is PPARγ-dependent, as demonstrated by PPARγ specific inhibitor. However, linkage between PPARγ and ERK/AKT phosphorylation is still not clear in this model. Indeed, increasing evidences suggested that natural and pharmacological PPARγ ligands induce rapid non-transcriptional effects in different cell types due to the extra-nuclear trafficking of PPARγ, and direct interaction of PPARγ with ERK and its upstream kinases [45]. In addition, ERK and AKT can be phosphorylated by several receptor tyrosine kinases (RTK) such as c-Met, EGFR, VEGFR or FGFR, and PPARγ has been demonstrated to interact with RTKs to phosphorylate ERK [46]. So, Rg_3 may activate RTKs through binding with PPARγ and subsequently activate the downstream ERK/AKT-eNOS signaling pathways.

Our previous study demonstrated that ginsenoside 20(R)-Rg_3 can reduce angiogenic activity of HUVECs by suppressing cell proliferation, chemoinvasion and MMPs expression [19]. The concentration of 20(R)-Rg_3 used in that study is in nanomolar level, which is different from the micromolar concentration used in the present study. It is not surprising that a single compound can act on different targets at different concentrations. Similar case was showed in genistein, the soy phytoestrogen, can activate estrogen receptor at low concentration (<μM) and inhibit adipogenesis; however, at high concentration (>μM), it promotes adipogenesis through acting as a ligand of PPARγ [47]. It may explain why the genistein functions only at certain level, as genistein plasma level of humans consuming diets without soy is only 40 nM, but can reach 4 μM in Japanese who consume large amount of soy products. This may also imply the contradictory activities of Rg_3 on modulating angiogenesis. If low concentration is applied, it may act on an unidentified target and exert its angiosuppressive effects; however, it may also promote angiogenesis at high concentration through binding to PPARγ. The plasma concentration of Rg3 can be varied, depends on the species and the amount of ginseng consumed, it can be ranged from nanomolar to micromolar level. As a result, the angiogenic effect of Rg3 may also vary. In addition to the concentration differences, the conditions of drug treatment may also lead to the different observation. The endothelial cells are treated in high serum concentration and are stimulated with VEGF,

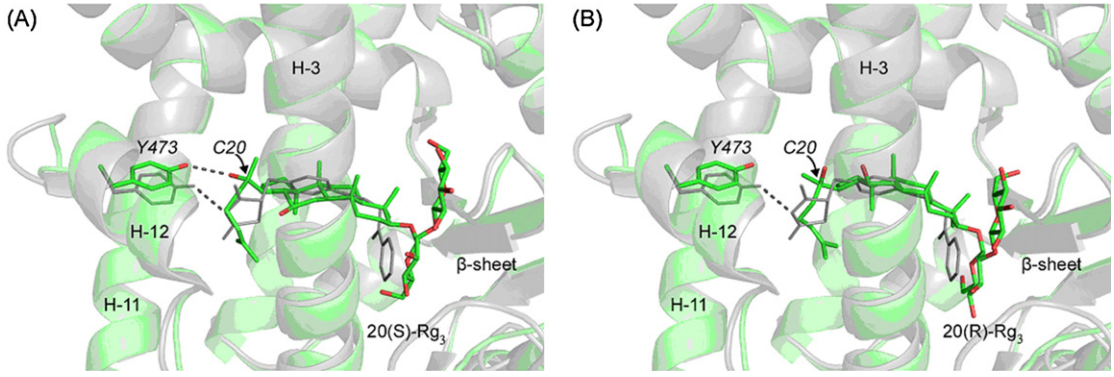

Fig. 6. Docking structures of 20(S)-Rg_3 and 20(R)-Rg_3 in the LBD of PPARγ. The ginsenosides and the side chain of Tyr473 in helix-12 (H-12) are shown in sticks. Crystal structure of rosiglitazone in PPARγ (PDB: 1ZGY) is superimposed and shown in gray for comparison. (A) The docked 20(S)-Rg_3 adopts a position similar of rosiglitazone in the protein and the hydroxyl group at the C20 position interacts with the side chain of Tyr473 (dotted line). (B) The docked 20(R)-Rg_3 occupies similar position as the 20(S)-Rg_3 in the protein but only the methyl group at the C20 position points towards Tyr473 and does not form any effective hydrogen bond. The protein backbones are rendered as faded out ribbons. Hydrogen atoms are not shown for clarity. Both Rg_3 stereoisomers were docked into the protein by using Autodock 4.0 [24], while the receptor protein structure is directly obtained from the protein databank (PDB: 2I4J) [25].

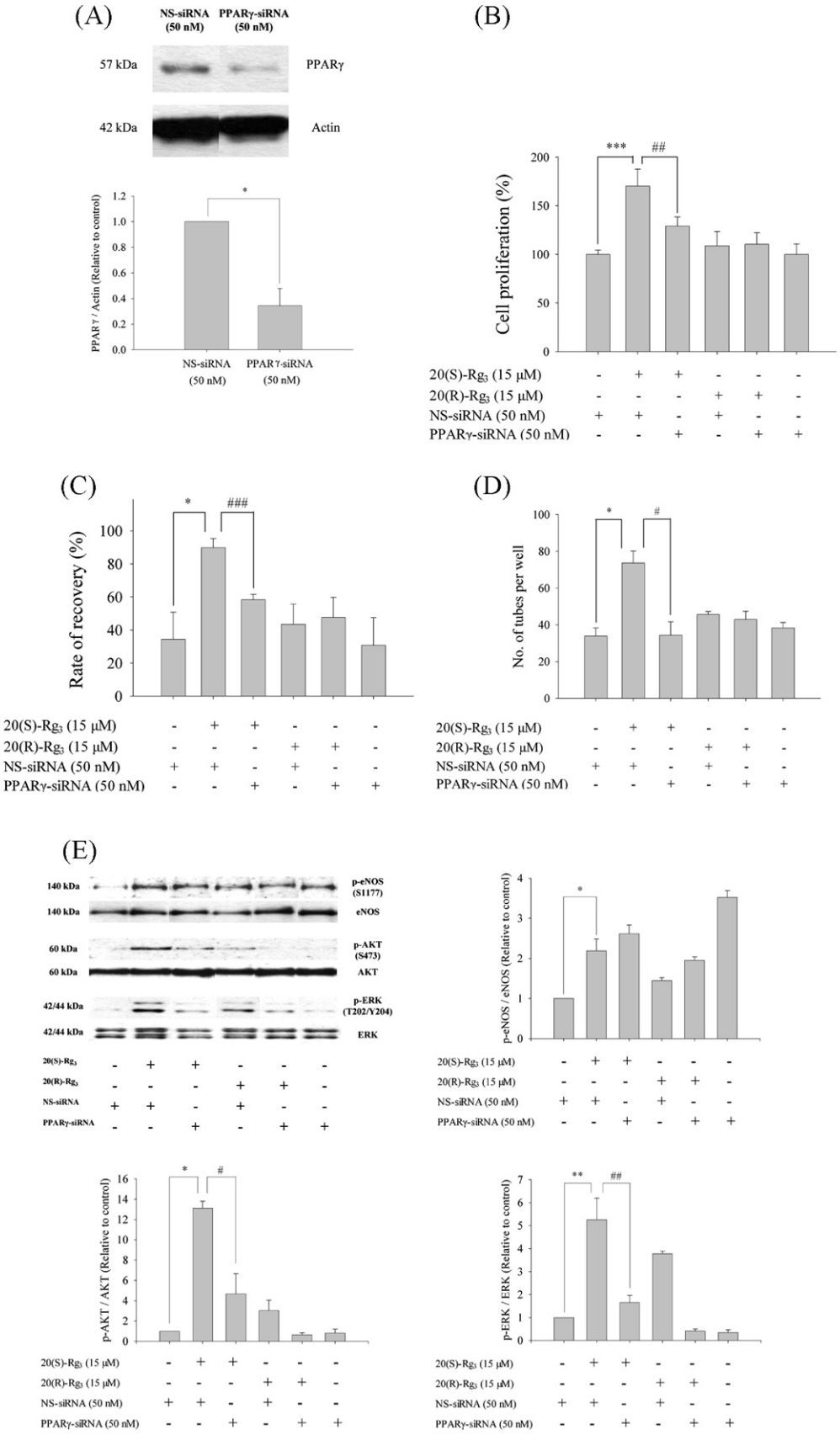

Fig. 7. Rg_3 induced angiogenic effects are dependent on PPARγ activation. HUVECs were transiently transfected with PPARγ-siRNA (50 nM) for 24 h before treatment of ginsenosides. (A) PPARγ-siRNA inhibited PPARγ protein expression. Signal intensities were determined by quantitative densitometry and expressed as fold change of PPARγ normalized to actin before compare with control. PPARγ-siRNA abolished 20(S)-Rg_3-induced (B) HUVECs proliferation, (C) HUVECs migration, (D) tube formation and (E) eNOS, AKT and ERK phosphorylation. Signal intensities were determined by quantitative densitometry and expressed as fold change of p-eNOS, p-AKT and p-ERK1/2 normalized to corresponding total form before compare with control. Values are presented as mean ± SD of three independent experiments. $^{*}p < 0.05$, $^{**}p < 0.01$, $^{***}p < 0.001$ vs DMSO control. $^{\#}p < 0.05$, $^{\#\#}p < 0.01$, $^{\#\#\#}p < 0.001$ vs 20(S)-Rg_3 treatment alone.

which mimic the tumor angiogenesis condition in the previous study. But in the present study, endothelial cells are treated with low serum concentration, which may resemble the normal and non-activated status (quiescence) of endothelial cells. So, ginsenoside Rg_3 may suppress angiogenesis when endothelial cells are activated, but may promote angiogenesis when the cells are unstimulated.

In summary, ginsenoside stereoisomers 20(S)-Rg_3 and 20(R)-Rg_3 differentially induce angiogenesis, in which 20(S)-Rg_3 significantly induces HUVECs proliferation, cell migration and tube formation, while 20(R)-Rg_3 has no effect. The underlying mechanisms may due to the differential activation of PPARγ and the downstream ERK/AKT-eNOS signaling. This study can enhance our understanding on the importance of ginsenoside stereochemistry and the angiogenic activity of Rg_3. More importantly, the results stress the slight structural difference between two ginsenoside stereoisomers can lead to significant differential physiological outcomes which should be carefully considered in the future development of ginsenoside-based therapeutics.

Conflict of interest

None declared

Acknowledgments

The authors thank Dr. Joshua K.K. Ko (School of Chinese Medicine, Hong Kong Baptist University) for providing PPARγ and RXRα expression vectors, and Dr. Bruce Spiegelman (Dana-Farber Cancer Institute, Harvard Medical School) for donating PPRE vector to Addgene. This work was supported by the General Research Fund (HKBU 261810), Research Grants Council, Hong Kong SAR Government, Strategic Development Fund, Hong Kong Baptist University, and AoE Funding (AoE/M-06/08) from the Area of Excellence Scheme of the University Grants Committee, Hong Kong SAR Government.

Appendix A. Supplementary data

Supplementary data associated with this article can be found, in the online version, at doi:10.1016/j.bcp.2011.12.039.

References

[1] Shibata S, Fujita M, Itokawa H, Tanako O, Ishii T. Studies on the constituents of Japanese and Chinese Crude Drugs, XI, Panaxadiol, a sapogenin of ginseng roots. Chem Pharm Bull (Tokyo) 1963;11:759–61.
[2] Kim WY, Kim JM, Han SB, Lee SK, Kim ND, Park MK, et al. Steaming of ginseng at high temperature enhances biological activity. J Nat Prod 2000;63:1702–4.
[3] Cheng L, Na JR, Bangm MH, Kim MK, Yang DC. Conversion of major ginsenoside Rb_1 to 20(S)-ginsenoside Rg_3 by *Microbacterium* sp. GS514. Phytochemistry 2007;69:218–24.
[4] Jeong SM, Lee JH, Kim JH, Lee BH, Yoon IS, Lee JH, et al. Stereospecificity of ginsenoside Rg_3 action on ion channels. Mol Cells 2004;18:383–9.
[5] Kim JH, Lee JH, Jeong SM, Lee BH, Yoon IS, Lee JH, et al. Stereospecificity effects of ginsenoside Rg_3 epimers on swine coronary artery contractions. Biol Pharm Bull 2006;29:365–70.
[6] Liu J, Shimizu K, Yu H, Zhang C, Jin F, Kondo R. Stereospecificity of hydroxyl group at C-20 in antiproliferative action of ginsenoside Rh_2 on prostate cancer cells. Fitoterapia 2010;81:902–5.
[7] Liu J, Shiono J, Shimizu K, Yu H, Zhang C, Jin F, et al. 20(R)-ginsenoside Rh_2, not 20(S), is a selective osteoclastgenesis inhibition without any cytotoxicity. Bioorg Med Chem Lett 2009;19:3320–3.
[8] Min JK, Kim JH, Cho YL, Maeng YS, Lee SJ, Pyun BJ, et al. 20(S)-ginsenoside Rg_3 prevents endothelial cell apoptosis via inhibition of a mitochondrial caspase pathway. Biochem Biophys Res Commun 2006;349:987–94.
[9] Lee YJ, Chung E, Lee KY, Lee YH, Huh B, Lee SK. Ginsenoside-Rg1, one of the major active molecules from *Panax ginseng*, is a functional ligand of glucocortocoid receptor. Mol Cell Endocrinol 1997;133:135–40.
[10] Hwang YP, Jeong HG. Ginsenoside Rb_1 protects against 6-hydroxydopamine-induced oxidative stress by increasing heme oxygenase-1 expression through an estrogen receptor-related PI3K/AKT/Nrf2-dependent pathway in human dopaminergic cells. Toxicol Appl Pharmacol 2010;242:18–28.
[11] Hwang JT, Lee MS, Kim HJ, Sung MJ, Kim HY, Kim MS, et al. Antiobesity effect of ginsenoside Rg_3 involves the AMPK and PPAR-gamma signal pathways. Phytother Res 2009;23:262–6.
[12] Duan SZ, Usher MG, Mortensen RM. PPARs: the vasculature, inflammation and hypertension. Curr Opin Nephrol Hypertens 2009;18:128–33.
[13] Liang C, Ren Y, Tan H, He Z, Jiang Q, Wu J, et al. Rosiglitazone via upregulation of AKT/eNOS pathways attenuates dysfunction of endothelial progenitor cells, induced by advanced glycation end products. Br J Pharmacol 2009;158:1865–73.
[14] Chu K, Lee ST, Koo JS, Jung KH, Kim EH, Sinn DI, et al. Peroxisome proliferator-activated receptor-gamma-agonist, rosiglitazone, promotes angiogenesis after focal cerebral ischemia. Brain Res 2006;1093:208–18.
[15] Cho D, Choi YJ, Jo SA, Jo I. Nitric oxide production and regulation of endothelial nitric-oxide synthase phosphorylation by prolonged treatment with troglitazone. J Biol Chem 2004;279:2499–506.
[16] Folkman J. Tumor angiogenesis: therapeutic implications. N Engl J Med 1971;285:1182–6.
[17] Roskoski Jr R. Vascular endothelial (VEGF) signaling in tumor progression. Crit Rev Oncol Hematol 2007;62:179–213.
[18] Yue PY, Leung EP, Mak NK, Wong RN. A simplified method for quantifying cell migration/wound healing in 96-well plates. J Biomol Screen 2010;15:427–33.
[19] Yue PY, Wong DY, Wu PK, Leung PY, Mak NK, Yeung HW, et al. The angiosuppressive effects of 20(R)-ginsenoside Rg_3. Biochem Pharmacol 2006;72:437–45.
[20] Nolte RT, Wisely GB, Westin S, Cobb JE, Lambert MH, Kurokawa R, et al. Ligand binding and co-activator assembly of the peroxisome proliferator-activated receptor-γ. Nature 1998;395:137–43.
[21] Li Y, Choi M, Suino K, Kovach A, Daugherty J, Kliewer A, et al. Structural and biochemical basis for selective repression of the orphan nuclear receptor liver receptor homolog 1 by small heterodimer partner. Proc Natl Acad Sci USA 2005;102:9505–10.
[22] Li Y, Kovach A, Suino-Powell K, Martynowski D, Xu HE. Structural and biochemical basis for the binding selectivity of peroxisome proliferator-activated receptor γ to PGC-1α. J Biol Chem 2008;283:19132–9.
[23] Einstein M, Akiyama TE, Castriota GA, Wang CF, McKeever B, Mosley RT, et al. The differential interactions of peroxisome proliferator-activated receptor (ligands with Tyr473 is a physical basis for their unique biological activities. Mol Pharmacol 2008;73:62–74.
[24] Morris GM, Goodsell DS, Halliday RS, Huey R, Hart WE, Belew RK, et al. Automated docking using a Lamarckian genetic algorithm and an empirical binding free energy function. J Comput Chem 1998;19:1639–62.
[25] Pochetti G, Godio C, Mitro N, Caruso D, Galmozzi A, Scurati S, et al. Insights into the mechanism of partial agonism: crystal structures of the peroxisome proliferator-activated receptor (ligand-binding domain in the complex with two enantiomeric ligands. J Biol Chem 2007;282:17314–2.
[26] Kim SM, Lee SY, Son SM, Choi SS, Yun YP, Yoo HS, et al. Combination of ginsenoside Rg_3 with docetaxel enhances the susceptibility of prostate cancer cells via inhibition of NF-kappaB. Eur J Pharamcol 2010;631:1–9.
[27] Musende AG, Eberding A, Wood C, Adomat H, Fazli L, Hurtado-Coll A, et al. Preclinical evaluation of Rh_2 in PC-3 human xenograft model for prostate cancer in vivo: formulation, pharmacokinetics, biodistribution and efficacy. Cancer Chemother Pharmacol 2009;64:1085–95.
[28] Park EK, Choo MK, Han MJ, Han MJ, Kim DJ. Ginsenoside Rh_1 possesses antiallergic and anti-inflammatory activities. Int Arch Allergy Immunol 2004;133:113–20.
[29] Zhang G, Liu A, Zhou Y, San X, Jin T, Jin Y. *Panax ginseng* ginsenoside-Rg2 protects memory impairment via anti-apoptosis in a rat model with vascular dementia. J Enthnopharmacol 2008;115:441–8.
[30] Brocks DR. Drug disposition in three dimensions: an update on stereoselectivity in pharmacokinetics. Biopharm Drug Dispos 2008;127:387–406.
[31] Campo VL, Bernardes LSC, Carvalho I. Stereoselectivity in drug metabolism: molecular mechanisms and analytical methods. Curr Drug Metab 2009;10:188–205.
[32] McConathy J, Owens MJ. Stereochemistry and drug action. Primary care companion. J Clin Psychiatry 2003;5:70–3.
[33] Jamali F, Mehvar R, Pasutto M. Enantioselective aspects of drug action and disposition: therapeutic pitfalls. J Pharm Sci 1989;78:695–715.
[34] Gu Y, Wang GJ, Wu XL, Zheng YT, Zhang JW, Ai H, et al. Intestinal absorption mechanisms of ginsenoside Rh_2: stereoselectivity and involvement of ABC transporters. Xenobiotica 2010;40:602–12.
[35] Fracchiolla G, Laghezza A, Piemontese L, Carbonara G, Lavecchi A, Tortorella P, et al. Synthesis, biological evaluation, and molecular modeling investigation of chrial phenoxyacetic acid analogues with PPARalpha and PPARgamma agonist activity. ChemMedChem 2007;2:641–54.
[36] Kwok K, Cheung N. Measuring binding kinetics of ligands with tethered receptors by fluorescence polarization and total internal reflection fluorescence. Anal Chem 2010;82:3819–25.
[37] Kim E, Surh Y. The role of 15-deoxy-$\Delta^{12,14}$-prostaglandin J_2, an endogenous ligand of peroxisome proliferator-activated receptor γ, in tumor angiogenesis. Biochem Pharm 2008;76:1544–53.
[38] Lee H, Gonzalez FJ, Yoon M. Ginsenoside Rf a component of ginseng, regulates lipoprotein metabolism through peroxisome proliferator-activated receptor alpha. Biochem Biophys Res Commun 2006;339:196–203.
[39] Hwang JT, Kim SH, Lee MS, Kim SH, Yang HJ, Kim MJ, et al. Anti-obesity effects of ginsenoside Rh_2 are associated with the activation of AMPK signaling pathway in 3T3-L1. Biochem Biophys Res Commun 2007;364: 1002–8.

[40] Han KL, Jung MH, Sohn JH, Hwang JK. Ginsenoside 20S-protopanaxatriol (PPT) activates peroxisome proliferator-activated receptor gamma (PPARgamma) in 3T3-L1 adipocytes. Biol Pharm Bull 2006;29:110–3.
[41] Nissen SE, Wolski K. Effect of rosiglitazone on the risk of myocardial infraction and death from cardiovascular causes. N Engl J Med 2007;356: 2457–571.
[42] Hien TT, Kim ND, Pokharel YR, Oh SJ, Lee MY, Kang KW. Ginsenoside Rg_3 increases nitric oxide production via increases in phosphorylation and expression of endothelial nitric oxide synthase: essential roles of estrogen receptor-dependent PI3-kinase and AMP-activated protein kinase. Toxicol Appl Pharmacol 2010;246:171–83.
[43] Bernier SG, Haldar S, Michel T. Bradykinin-regulated interactions of the mitogen-activated protein kinase pathway with the endothelial nitric-oxide synthase. J Biol Chem 2000;275:30707–15.
[44] Kim YM, Namkoong S, Yun YG, Hong HD, Lee YC, Ha KS, et al. Water extract of Korean red ginseng stimulates angiogenesis by activating the PI3K/Akt-dependent ERK1/2 and eNOS pathways in human umbilical vein endothelial cells. Biol Pharm Bull 2007;30:1674–9.
[45] Luconi M, Cantini G, Serio M. Peroxisome proliferator-activated receptor gamma (PPAR(): Is the genomic activity the only answer. Steroids 2010;75: 585–94.
[46] Tencer L, Burgermeister E, Ebert MP, Liscovitch M. Rosiglitazone induces caveolin-1 by PPARgamma-dependent and PPRE-independent mechanisms: the role of EGF receptor signaling and its effect on cancer cell drug resistance. Anticancer Res 2008;28:895–906.
[47] Dang ZC, Audinot V, Papapoulous SE, Boutin JA, Löwik CW. Peroxisome proliferator-activated receptor gamma (PPARgamma) as a molecular target for the soy phytoestrogen genistein. J Biol Chem 2003;278:962–7.